Chirality of Coiled Coils: Elasticity Matters

Sébastien Neukirch
Institut Jean le Rond d'Alembert, CNRS & Université Pierre et Marie Curie, Paris, France

Alain Goriely
Department of Mathematics and Program in Applied Mathematics, University of Arizona, Tucson, Arizona 85721, USA

Andrew C. Hausrath
Department of Biochemistry and Molecular Biophysics, University of Arizona, Tucson, Arizona 85721, USA
(Received 27 May 2007; published 25 January 2008)

Coiled coils are important protein-protein interaction motifs with high specificity that are used to assemble macromolecular complexes. Their simple geometric organization, consisting of α helices wrapped around each other, confers remarkable mechanical properties. A geometrical and mechanical continuous model taking into account sequence effects and based on the superhelical winding of the constituent helices is introduced, and a continuous family of solutions in which the oligomerization interactions are satisfied is derived. From these solutions, geometric and structural properties, such as the chirality and pitch of the coiled coil and the location of residues, are obtained. The theoretical predictions are compared to x-ray data from the leucine zipper motif.

DOI: 10.1103/PhysRevLett.100.038105 PACS numbers: 87.15.La, 36.20.−r, 62.20.D−

Coiled coils consist of α helices wound together to form a ropelike structure stabilized by hydrophobic interactions. The coiled-coil motif is found in about 10% of the proteins in the human genome [1]. Particular examples of coiled coils are keratin and the muscle protein tropomyosin. The widespread appearance of this motif is due in part to the simplicity, versatility, and economy by which coiled-coil forming sequences can achieve high specificity to select particular binding partners from a large choice of similar sequences, and in part to their mechanical properties. A coiled coil can extend and twist to store elastic energy and, accordingly, produce mechanical work. Whereas α helices are right handed, the overall chirality of most coiled coils built out of α helices, such as keratin, is left handed. This difference was first observed by Crick [2] who gave a geometric construction to reproduce both the handedness of keratin fibers and its global structure. Crick's construction was later generalized by Fraser and MacRae [3] who provided a formula for the pitch of a general coiled coil based on the periodicity of hydrophobic residues in the sequence. Absent from these analyses is a justification of this formula, a convincing explanation of the origin of the coiled-coil chirality, and the response of coiled coils under mechanical loads. The purpose of this Letter is to model the relation between structure and mechanical properties of coiled coils. We introduce a continuum representation that takes into account sequence effects and model the long-range elasticity of the structure. We assume that the coiled coils are in a canonical shape where the central axis of each α helix is itself a helix. We show that within the coiled-coil structure, all residues lie on helices. Further, there exists a continuum of possible structures with both chiralities satisfying the geometric requirements that the hydrophobic sides of the helices face each other, thereby disqualifying previous explanations [2,3] of chirality. The selection of a specific structure within this continuum and therefore its chirality is achieved by taking into account the mechanical energy of deformation for each structure.

Coiled coils are made out of *primitive helices* wound around each other; e.g., in a keratin dimer there are two primitive helices, which are α helices. We parametrize these structures in terms of curves on which residues lie at discrete points. Consider a curve $\mathbf{r}(s) = (x, y, z)$ parametrized by its arclength s in the three-dimensional space with fixed reference frame $\{\mathbf{e_x}, \mathbf{e_y}, \mathbf{e_z}\}$. We use the Cosserat moving frame $\{\mathbf{d_1}, \mathbf{d_2}, \mathbf{d_3}\}$, which is a right-handed orthonormal basis, built from the tangent director $\mathbf{d_3}(s) \equiv \mathbf{t}(s) = \mathbf{r}' = d\mathbf{r}/ds$. The two remaining directors $\mathbf{d_1}(s)$ and $\mathbf{d_2}(s)$ lie in the plane spanned by the usual normal $\mathbf{n}(s)$ and binormal $\mathbf{b}(s)$ vectors. The basis evolves according to $\mathbf{d}_i' = \boldsymbol{\kappa} \times \mathbf{d}_i$, $i = 1, 2, 3$, where $\boldsymbol{\kappa} = (\kappa_1, \kappa_2, \kappa_3)$ is the vector of material curvatures, related to the geometric curvature κ and torsion τ by $(\kappa_1, \kappa_2, \kappa_3) = (-\kappa\cos\phi, \kappa\sin\phi, \tau + \phi')$, where ϕ' is the excess twist [4], describing the material twist of a filament superimposed on its torsion. That is, the angle between the normal and the vector $d_1 = \mathbf{n}\sin\phi - \mathbf{b}\cos\phi$.

Polypeptide sequences that specify α-helical coiled coils can be characterized by sequence elements [5] with periodicity p. One prominent class is recognized by a heptad repeat motif [6] where $p = 7$. Positions of the residues within the heptad are labeled A through G, with positions A and D typically occupied by hydrophobic residues. These hydrophobic sites lie along a twisted hydrophobic strip that drives its association with another similar helix. To maximize the burial of these residues,

the primitive helix is distorted, introducing a bending of the helical axis and a twisting about this axis, which affects the disposition of the side chains. We first consider the positions of the residues on a canonical α helix, which is modeled as an elastic filament. The axis of the α helix is identified with the *center line* of the filament and the residues at positions $A, B, \ldots, G$ all lie on a cylinder of radius ρ; see Fig. 1. When the filament is straight and unstressed, i.e., the idealized form of an α helix, the center line of the filament is the z axis and the director frame for the filament is $\{\mathbf{d_1}, \mathbf{d_2}, \mathbf{d_3} \equiv \mathbf{t}\} = \{\mathbf{e_x}, \mathbf{e_y}, \mathbf{e_z}\}$. The residues A and D provide the interaction strip defined by two curves, respectively, joining the A and D residues (see Fig. 1). The *interface curve* is the center of this strip. On the cylinder representing the idealized α helix, the interface curve for a heptad repeat is a left-handed helix. With respect to the center line $\mathbf{r}(s)$ of the filament, this helix is defined by the material line:

$$\mathbf{d}_{\mathbf{hp}}(s) = \cos(\hat{\tau}s)\mathbf{d_1}(s) + \sin(\hat{\tau}s)\mathbf{d_2}(s). \quad (1)$$

The twist $\hat{\tau}$ is an intrinsic filament property defined by the periodicity of hydrophobic residues. To compute $\hat{\tau}$, we observe that there are 3.6 residues in every α-helix turn, that is, an angle $\alpha = 2\pi/3.6 = 5\pi/9 = 100°$ between residue. Each A residue has an angular offset of $-\pi/9$ radians with respect to the previous A residue. Since the rise per residue is $h_0 = 1.5$ Å, we have $\hat{\tau} = -\pi/9/(7 \times 1.5) \simeq -0.033$ rad/Å. In general, let α be the angle between each residue (positive if the primitive helix is right handed, negative otherwise), p the periodicity, then

$$\hat{\tau} = \frac{-\pi + (\alpha p + \pi) \mathrm{mod} 2\pi}{p h_0}. \quad (2)$$

The sign of $\hat{\tau}$ gives the chirality of the interface curve.

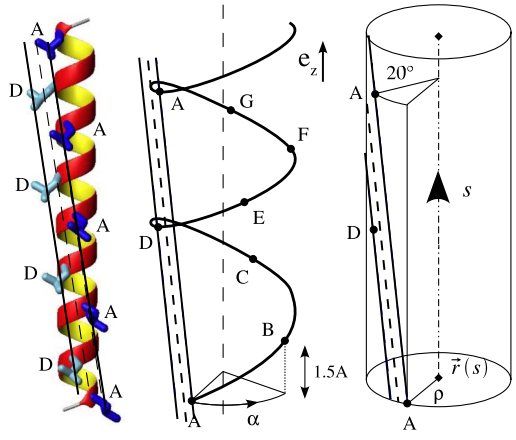

FIG. 1 (color online). Left: Idealized α helix with hydrophobic side chains at position A and position D in a heptad repeat. Middle: The primitive α helix. Right: The imaginary cylinder with residues lying at position $A, B, \ldots, G$ with hydrophobic strip (solid double line) and interface curve (dashed line).

We now consider a canonical *superhelix*, that is, a configuration where the center line $\mathbf{r}(s)$ of the filament is itself a helix, of radius R, axis $\mathbf{e_z}$, and pitch $2\pi R/\tan\theta$ [the *helical angle* θ is the angle between the tangent $\mathbf{t}(s)$ and the superhelical axis $\mathbf{e_z}$; see Fig. 2]. The center line of the filament in the superhelical configuration is $\mathbf{r}(s) = (+R\sin\psi(s), -R\cos\psi(s), s\cos\theta + z_0)$, where $\psi(s) = (\sin\theta)s/R + \psi_0$ is the equatorial angle, in the (x, y) plane, perpendicular to the axis of the superhelix. The (constant) curvature and torsion of the superhelix are $\kappa = \sin^2\theta/R$ and $\tau = \sin\theta\cos\theta/R$. The normal $\mathbf{n}(s)$ always faces toward the superhelical axis. The force that holds two (a dimer) or more α helices to coil around each other is the hydrophobic interaction. In these superhelical structures hydrophobic residues are sequestered from the solvent by clustering in the coil interior. In the case of dimers, symmetry implies that the hydrophobic residues face toward the superhelical axis. This fact can be expressed geometrically by requiring that in the superhelical configuration $\mathbf{d}_{\mathbf{hp}}(s) = -\mathbf{n}(s)$, $\forall\ s$. Using Eq. (1), we have

$$\cos(\hat{\tau}s + \phi) = 0, \forall\ s, \qquad \text{hence } \phi(s) = \pi/2 - \hat{\tau}s. \quad (3)$$

We conclude that the excess twist $\phi'(s)$ in the superhelical configuration is the opposite of the intrinsic twist $\hat{\tau}$ of the hydrophobic strip in the undistorted α-helix structure. In the general case of n primitive filaments, the hydrophobic residues do not necessarily face the central axis. Nevertheless, rotational symmetry of the structure (with primitive filaments identical to each other up to a rotation) leads to interface curves facing a prescribed direction (see Fig. 4 of [7]), which implies, again, that $\phi'(s) = -\hat{\tau}$. This last condition has another unforeseen consequence.

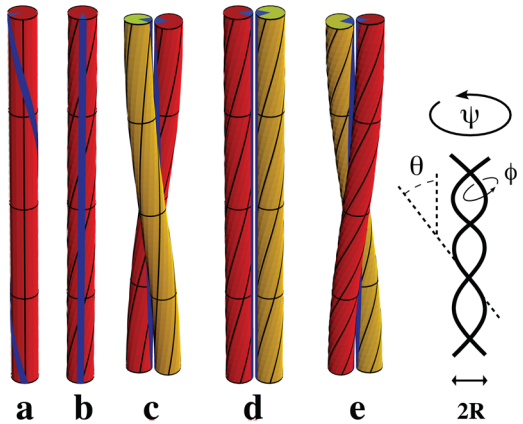

FIG. 2 (color online). (a) Undistorted filament with twisted hydrophobic strip, (b) filament twisted in such a way that the hydrophobic strip is straight, (c) left-handed coiled coil with two facing hydrophobic strips ($\theta = -0.1$ rad), (d) two parallel twisted filaments ($\theta = 0$), (e) right-handed coiled coil with two facing hydrophobic strips ($\theta = +0.1$ rad). In the last three configurations, the interface curve faces inward. Note that the twist (black lines on the filaments) is lower in the left-handed case.

All A residues lie on a helix of radius R_A with $R_A^2 = (R - \rho\cos\pi/7)^2 + \rho^2\cos^2\theta\sin^2\pi/7$, and helical angle θ_A given by $\tan\theta_A = (R_A/R)\tan\theta$. Similarly, all other residues (B through G) lie on (different) helices. Remarkably, there is no condition either on the superhelical angle θ or on the superhelical radius R. That is, for a given value of R, there exists a one-parameter continuous family of coiled coils parametrized by the superhelical angle θ, which all satisfy the hydrophobic constraint, as seen in Fig. 2. Hence, despite the conventional wisdom based on [2,3], the chirality of a coiled coil (given by the sign of θ) cannot be solely determined from the geometric properties of the hydrophobic strip of the primitive helices. A selection mechanism is now discussed.

Based on this geometric construction, we consider the mechanical aspects of the structures. We analyze the predicted conformations of the structure in the relaxed (unstressed) state and under external axial loads. To begin, we consider n identical primitive α helices as elastic filaments of length L that are naturally straight and untwisted. To form a coiled coil, an α helix will have to bend and twist, but for simplicity in the following treatment, we assume the primitive filaments to be inextensible. We also assume that when the n primitive filaments coil around one another, the energy associated with the hydrophobic interactions is much larger than the one associated with the elastic deformations [an estimate based on [8] gives $E_{\text{hydro}} = 5.1kT$ per residue, to be compared to $E_{\text{elas}} = 0.16kT$ per residue (computed with values from Table I)]. Thus, the hydrophobic interface is rigidly maintained and the geometric constraint (3) specifies the function $\phi(s)$. The energy cost associated with the elastic deformations of each filament can be written, phenomenologically, as the sum of the square of the three material curvatures

$$E_{\text{el}} = \frac{1}{2} n \int_0^L (B_1\kappa_1^2 + B_2\kappa_2^2 + B_3\kappa_3^2) ds, \tag{4}$$

where $B_1(s)$, $B_2(s)$ are the (local) bending rigidities along $\mathbf{d_1}$, $\mathbf{d_2}$ and $B_3(s)$ is the twist rigidity. For long deformations taking place over many residues, the bending and twisting rigidities are averaged and replaced by effective constant rigidities $B_1^{\text{eff}} = B_2^{\text{eff}} = B$ and $B_3^{\text{eff}} = C$ [10]. Equation (4) is applicable to general conformations of an elastic rod, which can be specified by any values of the curvatures $\boldsymbol{\kappa}$. Here we consider the case where the center lines of the deformed filaments are helices and the superhelix has a fixed (known) radius R and a constant helical angle θ in which case $\kappa = \sin^2\theta/R$ and $\tau = \sin\theta\cos\theta/R$.

To the energy of elastic deformations E_{el} we add the work done by an external force F and torque M, which we consider acting along the superhelical axis $\mathbf{e_z}$. The total energy is $E = n\int_0^L V ds$ with

$$V = \frac{B}{2}\frac{\sin^4\theta}{R^2} + \frac{C}{2}\left(\frac{\sin 2\theta}{2R} - \hat{\tau}\right)^2 - \frac{F}{n}\cos\theta - \frac{M}{nR}\sin\theta. \tag{5}$$

With R constant, V depends only on θ, and a minimum in the energy is obtained when $dV/d\theta = 0$, that is,

$$2B\sin^3\theta\cos\theta + C\cos(2\theta)(\sin\theta\cos\theta - \hat{\tau}R) + R^2\frac{F}{n}\sin\theta - R\frac{M}{n}\cos\theta = 0. \tag{6}$$

The solution of this equation gives the superhelical angle θ as a function of the intrinsic parameters of the coiled structure (the rigidities B and C, and the twist $\hat{\tau}$ of the hydrophobic strip) when the structure undergoes tensile ($F \neq 0$) and torsional ($M \neq 0$) deformation. We first focus on the case with no external load ($F = 0 = M$). Then, the rest state is characterized by a superhelical angle $\theta = \theta_0$, solution of

$$-2(B/C)\sin^3\theta_0\cos\theta_0/\cos 2\theta_0 = \sin\theta_0\cos\theta_0 - \hat{\tau}R. \tag{7}$$

For small angles θ_0, the left-hand side is of order $O(\theta_0^3)$; hence,

$$\theta_0 \simeq \hat{\tau}R \quad \text{if } \theta_0 \ll 1. \tag{8}$$

A few comments are in order. First, an important consequence of Eq. (8) is that equilibrium requires that the chirality of the coiled structure (i.e., the sign of θ_0) is given by the chirality of the hydrophobic strip (i.e., the sign of $\hat{\tau}$) and not by the chirality of the primitive α helix. For example, in the case of an undecad repeat ($p = 11$), the hydrophobic strip on the primitive helix is right handed and the coiled coil formed is right handed as well [11]. Second, we remark that in the limit $B/C \to 0$ in Eq. (7), we recover Eq. (15.6), page 458 of [3] (with $P = 2\pi R/\tan\theta_0$, $\Delta t = \hat{\tau}h_0$, and $h = h_0\cos\theta_0$). This classic formula of the biochemistry literature is usually attributed to Fraser and MacRae [3] where it is given without derivation. Hence Eq. (7) can be seen as a correction to the empirical observation of Fraser and MacRae, but more importantly Eq. (6) is a generalization to the case where external loads are present. A different formula for the pitch of a coiled coil as a function of the twist $\hat{\tau}$ based also on elastic theory has been proposed in [12]. However, we disagree with their results. For instance, the limit $B/C \to 0$ of Eq. (7) leads (exactly and for all $\hat{\tau}$ and all θ_0) to Fraser and MacRae's formula, whereas the same limit of Eq. 9 in [12], does not recover the well-tested empirical law of Fraser and

TABLE I. Comparison of the superhelical angle (2θ) from x-ray data (see [9]) with Eq. (8). Radii and rises given in Å.

		X-ray data			Model	
Oligomer	Res./turn	Rise/res.	R	2θ	$\hat{\tau}$ (rad/Å)	2θ
Dimer	3.62	1.51	4.9	−23.4°	−0.039	−22°
Trimer	3.60	1.53	6.7	−26.8°	−0.033	−25°
Tetramer	3.59	1.52	7.6	−26.0°	−0.030	−26°

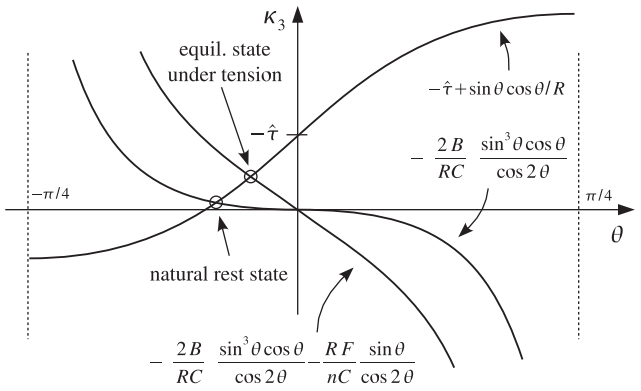

FIG. 3. The mechanical state of the superhelical configuration is at the intersection of the two curves describing the twist κ_3 in the protofilaments. In the tensile regime, the mechanical state is shifted toward smaller θ (in absolute values) and higher twist.

MacRae. The reason for this discrepancy stems from differences in the basic geometric assumptions; whereas [12] considers the averaged deformation of the middle line of the structure, we consider deformations of individual α helices. Note also that Eqs. (6) and (7) yield good agreement with experiments performed on elastic filaments [13] provided $\hat{\tau}$ is identified with a pretwist. Third, we remark that superhelical geometry implies a fundamental coupling between extension and rotation. Pulling on a structure changes its superhelical angle θ, which changes both its extension and its overall rotation. The deformation of coiled coils under external loads is given by Eq. (6) (see Fig. 3).

Structurally, the heptad repeat is the best characterized motif in the class of coiled coils, and there are numerous crystal structures of variant leucine zipper proteins. In order to test the validity of approximation (8), we use the crystal data provided in [9] to compare the experimental superhelical angle θ (as given by x-ray data) to the one computed by Eq. (8). The comparison in Table I shows good quantitative agreement.

This analysis of coiled coils is also directly applicable to other superhelical structures stabilized through other mechanisms. For instance, the triple helix of collagen, a right-handed superhelix, is held together by hydrogen bonds between the primitive collagen helices. Nevertheless, from a geometric and mechanical perspective, these superhelical structures can be treated in the same way as coiled coils. Each individual strand is a left-handed helix with a repeating motif of $p = 3$ residues: Gly-X-Y. The glycine residues have to face the interior of the structure (in this sense they play the same role as the hydrophobic residues in coiled coils). There are 10 residues per 3 turns, that is $\alpha = -3\pi/5$, which implies a positive shift of $\pi/5$ rad between glycine residues [14]. Equation (2) with a rise h_0 per residue of 2.86 Å yields $\hat{\tau} = 0.0732$ rad/Å. The positive sign confirms that the triple helix is right handed.

We introduced a continuum elastic model reconciling the mechanical and structural properties of coiled coils. The coiled coil is considered to comprise two or more elastic filaments that are uniform and isotropic in their elastic properties. The model explains how the observed chirality of the coiled coils is due to *both* the location of specific residues and the requirement that the constituent helices are at equilibrium in the coiled-coil configuration.

This material is based in part upon work supported by the National Science Foundation under Grants No. DMS-0604704 and No. DMS-IGMS-0623989 (A. G.) and a BIO5 Institute Grant (A. G., A. H.)

[1] A. Rose and I. Meier Cell Mol. Life Sci. **61**, 1996 (2004).
[2] F. H. C. Crick, Acta Crystallogr. **6**, 689 (1953).
[3] R. D. B. Fraser and T. P. MacRae, *Molecular Biology* (Academic Press, New York, 1973).
[4] A. E. H. Love, *A Treatise on the Mathematical Theory of Elasticity* (Dover, New York, 1944), 4th ed.
[5] M. Gruber and A. N. Lupas, Trends Biochem. Sci. **28**, 679 (2003).
[6] W. H. Landschulz, P. F. Johnson, and S. L. Mcknight, Science **240** 1759 (1988); E. K. Oshea, R. Rutkowski, and P. S. Kim, Science **243**, 538 (1989); L. Pauling, R. B. Corey, and H. R. Branson, Proc. Natl. Acad. Sci. U.S.A. **37**, 235 (1951).
[7] J. Liu *et al.*, Proc. Natl. Acad. Sci. U.S.A. **103**, 15457 (2006).
[8] C. Tanford, J. Am. Chem. Soc. **84**, 4240 (1962).
[9] P. B. Harbury, P. S. Kim, and T. Alber, Nature (London) **371**, 80 (1994).
[10] S. Kehrbaum and J. H. Maddocks, in *Proceedings of the 16th IMACS World Congress*, edited by M. Deville and R. Owens (IMACS, Lausanne, 2000), ISBN 3-9522075-1-9.
[11] J. Peters, W. Baumeister, and A. Lupas, J. Mol. Biol. **257**, 1031 (1996); A. Lupas, Trends Biochem. Sci. **21**, 375 (1996).
[12] C. W. Wolgemuth and S. X. Sun, Phys. Rev. Lett. **97**, 248101 (2006); S. Choe and S. X. Sun, J. Chem. Phys. **122**, 244912 (2005).
[13] J. M. T. Thompson, G. H. M. van der Heijden, and S. Neukirch, Proc. R. Soc. A **458**, 959 (2002).
[14] K. Beck and B. Brodsky, J. Struct. Biol. **122**, 17 (1998).